Morphology Changes in PCPDTBT:PCBM and P3HT:PCPDTBT:PCBM and its Effect on Polymer Solar Cell Performance

A Senior Project

presented to

the Faculty of the Physics Department

California Polytechnic State University, San Luis Obispo

In Partial Fulfillment

of the Requirements for the Degree

Bachelor of Science

by

Galen David Cauble

August, 2011

Abstract

Polymer solar cell morphology is sensitive to both heat and time. By thermally annealing polymer solar cells the morphology of the devices can be altered causing immediate changes in device performance. Blending PCPDTBT:PCBM with P3HT:PCPDTBT combines the absorption characteristics of each to create a more even absorption spectrum. Subjecting PCPDTBT:PCBM, and P3HT:PCPDTBT:PCBM polymer solar cells to thermal annealing as well as recording device performance through time has shown that P3HT:PCPDTBT:PCBM devices react positively to thermal annealing (increasing from 0.8% to 1.4%) while PCPDTBT:PCBM devices have varied reactions. Furthermore, the P3HT:PCPDTBT:PCBM devices have achieved efficiencies of 1.6% in AM 1.5 compared to 1.5% in PCPDTBT:PCBM devices.

Introduction

Polymer solar cells have the potential to be a low-cost and clean solar energy replacement to traditional fossil fuel sources. Their high absorptivity allows for ultra-thin devices compared to modern silicon solar cells with relatively low absorptivity; this helps decrease materials cost [1]. Furthermore, the polymer blends in these solar cells have characteristics similar to an ink and can thus be printed, allowing for easier mass-production [2].

Efficiency and lifetime are two major areas of interest for polymer solar cells. With relatively low efficiencies, compared to their silicon counterparts, polymer solar cells must continue to rise in efficiency to become competitive with traditional fuel sources. Furthermore, the devices are subject to external and internal degradation. The Polymer:PCBM layer as well as reactive metal cathodes, such as calcium, mean that if not properly packaged devices will be contaminated by water and oxygen. The PEDOT layer of the solar cells is also thought to be corrosive and further decreases the lifetime [3]. Different polymer blends as well as the changing morphology of these layers have important effects on device efficiency. These changes in morphology include growing

homogenous regions of Polymer and PCBM (spinodal decomposition), an evening of the internal layer of the device which helps eliminate micro-shorts, and crystallization of P3HT which increases absorptivity [4]. It should be noted that PCPDTBT is amorphous and thus does not crystalize [5]. In this report, the polymer fullerene blends, PCPDTBT:PCBM and P3HT:PCPDTBT:PCBM were investigated and subjected to thermal and sedentary annealing while their efficiencies were recorded.

Theory

For our investigation, polymer solar cell devices were made with Poly (3-hexylthiopene-2, 5-diyl) *P3HT* and/or poly[2,6-(4,4-bis-(2-ethylhexyl)-4H-cyclopenta[2,1-b;3,4-b]dithiophene)-alt-4,7-(2,1,3-benzothiadiazole)] *PCPDTBT*. These polymers are mixed with [6,6]-Phenyl-C61-butyric acid methyl ester *PCBM* which is simply a modified Bucky Ball with an attached tail to improve solubility. From here onwards when referring to the mixed Polymer:PCBM layer only the polymer will be listed, it is to be assumed that the polymer is mixed with PCBM unless clearly stated otherwise. Polymer solar cells work by first absorbing a photon into the polymer layer of the device. The photon excites an electron from its highest occupied molecular orbital (HOMO) to the lowest unoccupied molecular orbital (LUMO) state. This excited electron creates a positive hole where the electron is absent, resulting in what is known as an exciton, an electron-hole pair bound together to travel along the polymer layer [1].

The extraction of these charges is heavily affected by the morphology of the devices. Depending on the polymer, excitons have a mean diffusion distance before they recombine and halt charge extraction. This distance is about 10 nm, meaning that an ideal region size

is twice the mean diffusion distance [6]. Region size is affected by a number of factors including thermal annealing, solvents used to dissolve the polymer layer and their concentrations, and simply time [7].

If an exciton is able to come in contact with a heterojunction between the polymer and PCBM, the higher electronegativity of the PCBM will cause the exciton to dissociate. This process takes place on a femtosecond timescale [9]. The difference in work function of the device electrodes creates an internal electric field which will pull the electron and positive hole in different directions. Given an adequate pathway the electron will travel along the PCBM to the metal electrode (Calcium/Aluminum) and the positive hole along the polymer to the Indium-Tin-Oxide (ITO) electrode (Figure 1) [1].

Furthermore, devices can be made with a Poly(3,4-ethylenedioxythiophene) poly(styrenesulfonate) *PEDOT* layer between the polymer and anode electrode. This conducting layer increases the work function between the electrodes causing a rise in maximum possible voltage [1]. While PEDOT does help device performance it is not necessary for the devices to function.

Experimental Procedure

We fabricate our solar cells entirely in the Polymer Electronics Lab on the California Polytechnic San Luis Obispo campus. The process begins with a glass substrate covered in preprinted ITO pads (Figure 2a). To ensure the devices are clean we subject the substrates to an ultra-sonic bath in both acetone and isopropyl alcohol. We transfer the devices into a dust free area and further clean them in a UV Ozone machine. The ozone helps react with any organic material left on the devices after the baths and helps to diffuse oxygen into the ITO regions, extending its lifetime.

We cover the devices in PEDOT and spincoat them at 500 rpm for 60 seconds to help planarize the layer. We use distilled water to wipe the PEDOT from the edges of the substrates, as PEDOT is water soluble, to prevent shorting pathways between the metal electrode and ITO (Figure 2b). We heat the devices to 140 °C for 10 minutes to remove any excess water before we transport them into a clean nitrogen rich glove box to shield the devices from water and oxygen. We move the devices into the glove box while still hot to minimize the amount of water being brought into the glove box.

In the glove box we spincoat devices in a solution of polymer, PCBM, and solvent. This solution has pre-measured concentrations of each component and is allowed to dissolve with a magnetic spin bar for a minimum of 24 hours at 50 °C and 500 rpm. The PCPDTBT solution is 12mg/ml at a 1:3 ratio with PCBM, while the P3HT:PCPDTBT is a 1:1 mixture of the 12mg/ml PCPDTBT solution combined with a P3HT solution of 20mg/ml at a 1:1 ratio with PCBM. The solvent used for both solutions was Chlorobenzene. We created 11 PCPDTBT devices in the first run, in the second run we created 7 PCPDTBT and 5 P3HT:PCPDTBT devices. We apply the solution to the substrate and spin at specific speeds to vary thickness. We may then subject devices to thermal annealing to help speed spinodal decomposition, promote crystallization and eliminate micro-shorts [8]. The polymer layer is then wiped off the sides of the device, using a toluene swab, to allow appropriate contact on the outer electrodes (Figure 4c).

We then transport devices to a cleaner nitrogen rich environment to deposit the metal cathode. This metal cathode is actually comprised of two metals, aluminum and calcium. We then move the devices into a low pressure chamber, on the order of 10^{-7} Torr. The metals are evaporated (calcium sublimates) by running a high current through a

housing boat in which the metal is contained. The high current eventually causes the metal to evaporate and coat the solar cell. The calcium is deposited first and the aluminum afterwards in thicknesses of ~20 nm and ~80 nm respectively. The aluminum helps shield the calcium from any contact it may have with water or oxygen, while the calcium provides higher energy electrons to aid charge extraction. A shield is used to evaporate metal in four specific areas; this allows four unique solar cells or "pixels" on each substrate (Figure 2d). After cathode deposition the devices are ready to be tested.

The first round of testing takes place in the glove box using a Dolan Jenner lamp with a light intensity of 18 $\frac{\mathrm{W}}{\mathrm{m}^2}$. We place the devices in a jig which pushes gold pins against both electrodes of each of the four pixels. By measuring the current traveling through these pins and voltage across them we can calculate the devices power conversion efficiency and open circuit voltage. We measure the power conversion efficiency by first measuring the maximum power density (current density multiplied by voltage). The maximum power density is found by calculating the largest area created by a specific current and voltage on a J-V curve (Figure 4). The maximum electrical power output density is then divided by the input light power density. The resulting number is the power conversion efficiency of our devices, as demonstrated below:

$$Efficiency = \frac{Electrical\ Power_{max}}{Light\ Power_{input}} = \frac{0.35\ \mathrm{V} * 0.456\ \frac{\mathrm{A}}{\mathrm{m}^2}}{18\ \frac{\mathrm{W}}{\mathrm{m}^2}} * 100\% = 0.886\%.$$

Next we calculate the open circuit voltage by applying a voltage opposite the devices built in voltage, Voc (Figure 4). Once the current drops to zero we know we have perfectly balanced the devices maximum possible voltage. We then calculate the short circuit current, Jsc, by measuring the point at which voltage drops to zero with a sourced voltage

(Figure 4). The maximum power output density can be divided by the product of the short circuit current density and open circuit voltage. This result is called the Fill Factor and represents how well the device performs according to its theoretical maximum, as described below:

$$Fill\ Factor = \frac{Power_{max}}{Jsc * Voc} = \frac{0.35\ \text{V} * 0.456\ \frac{\text{A}}{\text{m}^2}}{7.87 * 10^{-1}\ \frac{\text{A}}{\text{m}^2} * 0.482\ \text{V}} * 100\% = 42\%.$$

Devices can be brought out into sunlight after they are packaged with aluminum tape sealed with epoxy. Devices degrade quickly even with the packaging meaning that further testing must take place immediately. The devices are taken out into direct sunlight at AM 1.5 (when light is passing through 1.5 air masses of atmosphere with 1 air mass being zenith and Air Mass 1.5 being 48.2° off zenith) where they are once again tested. This higher light intensity of $1000\ \frac{\text{W}}{\text{m}^2}$ allows us to see how well our devices would perform under realistic conditions.

By annealing our devices we can help to speed along spinodal decomposition and form crystalline structures in the P3HT. Figure 3, 5, and Table 6 show annealing specifications for various devices. The devices are transported back into polymer spin coating glove box and allowed to anneal on a hot plate. Temperature and time were both varied in order to find an optimum annealing time.

In order to test for absorption we use an ocean optics spectrometer to record the spectrum relative to a blank substrate's absorption. We test the two small pixels on each device to avoid damaging the big pixels (Figure 2d). Absorption data can show changes in crystalline structure of the P3HT.

Data

PCPDTBT Sedentary and Thermal Annealing

In our PCPDTBT only run the devices show a sharp increase in efficiency as the Voc increases (Figure 3a). The Voc continues to rise even with a subtle fall in Jsc, meaning efficiency continues to rise as well. The devices then peaked because of a drastic rise in Jsc. This same peak has not yet been seen in the second batch of PCPDTBT devices so it may be an error in testing, possibly due to a change in light sources. Even so, the peak is represented by three data points which lowers the possibility of simply a light source switch. After this peak the efficiency begins to decrease as Jsc lowers. The devices were then subjected to thermal annealing (Figure 3b and PCPDTBT devices from Figure 5b). In our first PCPDTBT run the devices begin to fall after consecutive annealing. Our second PCPDTBT run shows that devices remain constant or even slightly improve through annealing. A possible explanation could be that the first batch of PCPDTBT devices was made in the spring while the second was made during the summer. The solvent was thus allowed to dissolve the polymer and PCBM for much longer. This could mean that during the second batch the PCPDTBT devices may have started off with a less optimum morphology so initially annealing helped the devices undergo spinodal decomposition faster. The difference in age of the solution may have also accounted for the sharp rise in Jsc during the first PCPDTBT run.

P3HT:PCPDTBT Sedentary and Thermal Annealing

The P3HT:PCPDTBT devices show the characteristic initial rise apparent in PCPDTBT but also react strongly to thermal annealing (Figure 5b). Devices were annealed in accordance with Table 6. P3HT:PCPDTBT devices improved drastically to a point and

then began to fade. We experimented with different annealing times, stopping when devices began to degrade. Eventually we decided that ~25 minutes at 105/130 °C were appropriate annealing specifications. We tested this hypothesis by subjecting two P3HT:PCPDTBT devices (devices 5 and 6) to these annealing specifications. Both improved but the device annealed at 105 °C improved more (5 from 0.8% to 1.4% and 6 from 0.6% to 1.1%). This lead us to believe that higher temperature anneals on P3HT:PCPDTBT devices can do damage. We have noticed that after over-annealing P3HT:PCPDTBT devices to a lower efficiency they will sometimes "bounce back" to a higher efficiency. This could be explained by P3HT's tendency to crystallize. This means that even when forced out of an optimum crystalline structure due to high temperatures, it may have the ability to reform the crystalline structure given enough time.

P3HT:PCPDTBT Annealing, Absorption, and Crystallization

In order to show the crystallization of the P3HT we used P3HT:PCPDTBT devices from a failed device run. The devices failed most likely due to a contaminated calcium layer. Regardless of their failure as working solar cells, the polymer layer is still intact and can thus be tested for absorption. We annealed three devices which had different spin speeds and thus different thicknesses (800, 1600, and 2400 rpm). After each anneal we recorded the absorption (Figure 7a-c). It is apparent that as the P3HT:PCPDTBT devices are annealed the extra heat speeds along the development of P3HT crystalline structures as absorption from 500 to 600 nm increases dramatically. This is especially apparent in the thinner device as crystalline structures are much better at absorbing light than an amorphous layer of the same thickness, with absorption increasing by over 100% at certain wavelengths between 500 and 600 nm. The increase was not as apparent in the

parts of the spectrum covered by PCPDTBT (where absorption peaks at 650 to 800 nm and to a lesser extent 400 nm) as it is amorphous and thus does not crystallize.

AM 1.5 Testing

As an important measure of how well devices perform in a realistic environment AM 1.5 testing was done on both the PCPDTBT devices from the first run, the PCPDTBT devices from the second run, and the P3HT:PCPDTBT devices (Figure 8). In highlight the first PCPDTBT device and the P3HT:PCPDTBT devices performed the best, with the P3HT:PCPDTBT (device 10) hitting 1.6% efficiency and the PCPDTBT (device 11) at 1.5% efficiency (efficiencies were averaged across pixels in each device).

Conclusion

When subjected to thermal annealing PCPDTBT and P3HT:PCPDTBT devices both undergo morphology changes. While it is thought that PCPDTBT devices simply undergo spinodal decomposition at an accelerated rate and repair micro-shorts quicker, P3HT:PCPDTBT devices seem to improve drastically due to the crystallization of P3HT. This crystallization along with the morphology changes present in pure PCPDTBT devices has improved device efficiencies by 0.8% to 1.4% in our best P3HT:PCPDTBT device when annealed for 25 minutes at 105 °C. This rise in efficiency is due to greater absorption of light from the crystalline structure which has been seen to increase absorption by more than 100% at certain wavelengths between 500 and 600 nm.

Furthermore the P3HT:PCPDTBT seems to outperform its pure PCPDTBT counterpart in AM 1.5 conditions. While there are many dangers involved with packaging devices to test them in AM 1.5 this result is promising as the P3HT:PCPDTBT devices are currently un-optimized. Because the absorption spectrum of P3HT:PCPDTBT devices is a

combination of P3HT, PCPDTBT, and PCBM's absorption spectrum, work can be done in better balancing and "flattening" the current absorption spectrum. This would be done by varying the concentrations of polymer and PCBM in the solutions. The fact that P3HT:PCPDTBT creates a more even spectrum could be a reason it outperforms PCPDTBT in high light.

References

[1] Sean E. Shaheen and David S. Ginley, "Organic-Based Photovoltaics: Toward Low-Cost Power Generation," MRS Bulletin 30, 10-19 (2005).

[2] Schilinsky, P., Waldauf, C. and Brabec, C. (2006), Performance Analysis of Printed Bulk Heterojunction Solar Cells. Advanced Functional Materials, 16: 1669–1672. doi: 10.1002/adfm.200500581

[3] Kion Norrman, Morten V. Madsen, Suren A. Gevorgyan, and Frederik C. Krebs, "Degradation Patterns in Water and Oxygen of an Inverted Polymer Solar Cell," Journal of the American Chemical Society, VOL. 132, NO. 47, 2010

[4] Samuele Lilliu, Tiziano Agostinelli, Ellis Pires, Mark Hampton, Jenny Nelson, J. Emyr Macdonald "Dynamics of Crystallization and Disorder during Annealing of P3HT/PCBM Bulk Heterojunctions," Macromolecules 2011 44 (8), 2725-2734

[5] Gu, Yu; Russell, Thomas, "Studies on Morphology of PCPDTBT/Fullerene Bulk Heterojunction Organic Photovoltaics," American Physical Society, APS March Meeting 2011, March 21-25, 2011, abstract #C1.007

[6] Christoph J. Brabec, Gerald Zerza, Serdar Sariciftci, et al. "Tracing photoinduced electron transfer process in conjugated polymer/fullerene bulk heterojunctions in real time " Chemical Physics Letters 340, 232-236 (2001).

[7] Soci, C., Hwang, I.-W., Moses, D., Zhu, Z., Waller, D., Gaudiana, R., Brabec, C. and Heeger, A. (2007), Photoconductivity of a Low-Bandgap Conjugated Polymer. Advanced Functional Materials, 17: 632–636. doi: 10.1002/adfm.200600199

[8] Wanli Ma, Cuiying Yangand, Alan J. Heeger, et al. "Thermally Stable, Efficient Polymer Solar Cells with Nanoscale Control of the Interpenetrating Network Morphology," Adv. Funct. Mater. 15, 1617-1622 (2005).

[9] Xiaoniu Yang and, Joachim Loos, "Toward High-Performance Polymer Solar Cells: The Importance of Morphology Control," Macromolecules 2007 40 (5), 1353-1362

Figures

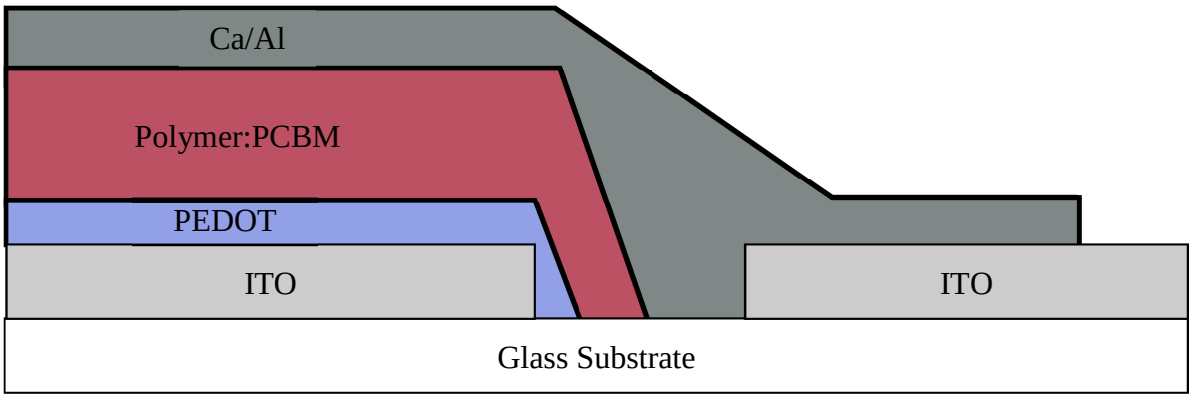

Figure 1 - A cross section of our devices, they are fabricated from bottom to top (Glass Substrate to Ca/Al cathode. This picture also shows the importance of wiping the Polymer:PCBM layer and PEDOT layer. Without wiping there would be a shorting pathway between the active layer ITO pad and the cathode. Additionally, without wiping the Polymer:PCBM layer adequate contact could not be made with the ITO.

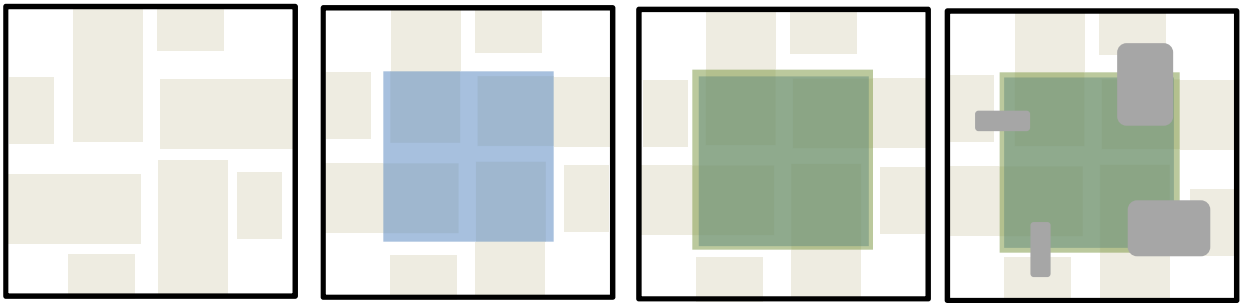

Figure 2 - Blank ITO, PEDOT layer, Polymer Layer, and Metal Cathode from left to right.

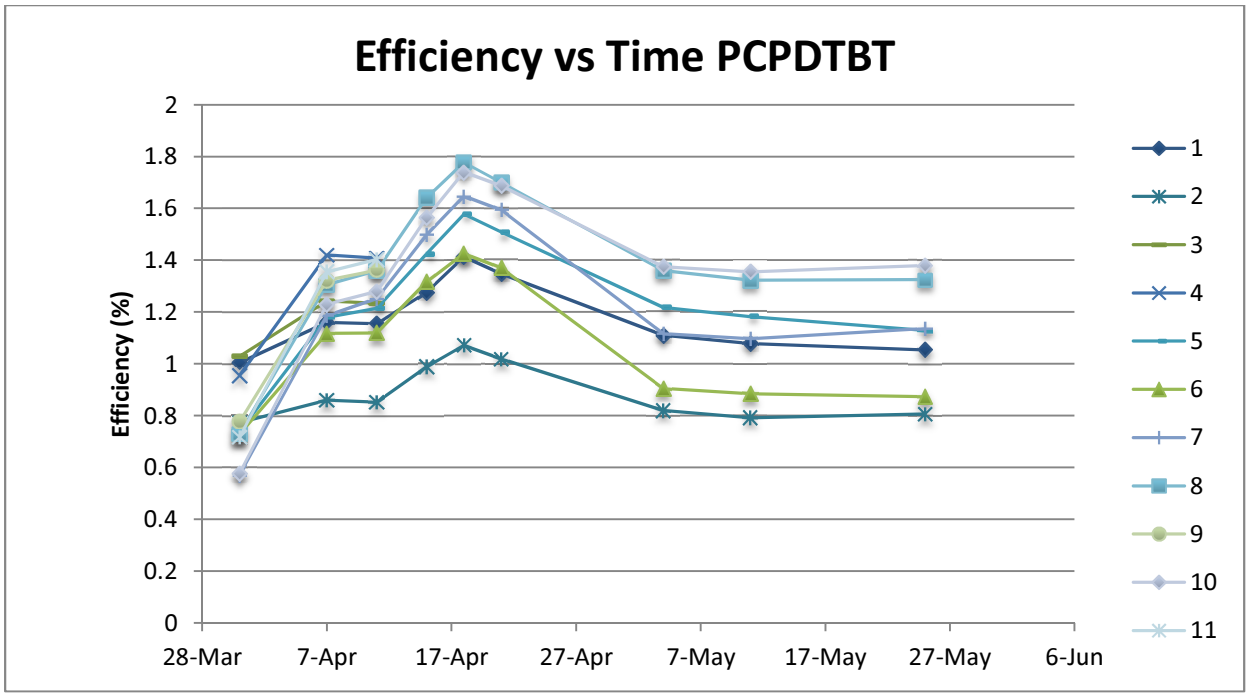

Figure 3a - The first PCPDTBT run showing efficiency through time. The initial rise is due to an increase in Voc, the second rise is due to a rise in Jsc which is currently unexplained. The devices begin to degrade as Jsc falls without any additional increase in Voc.

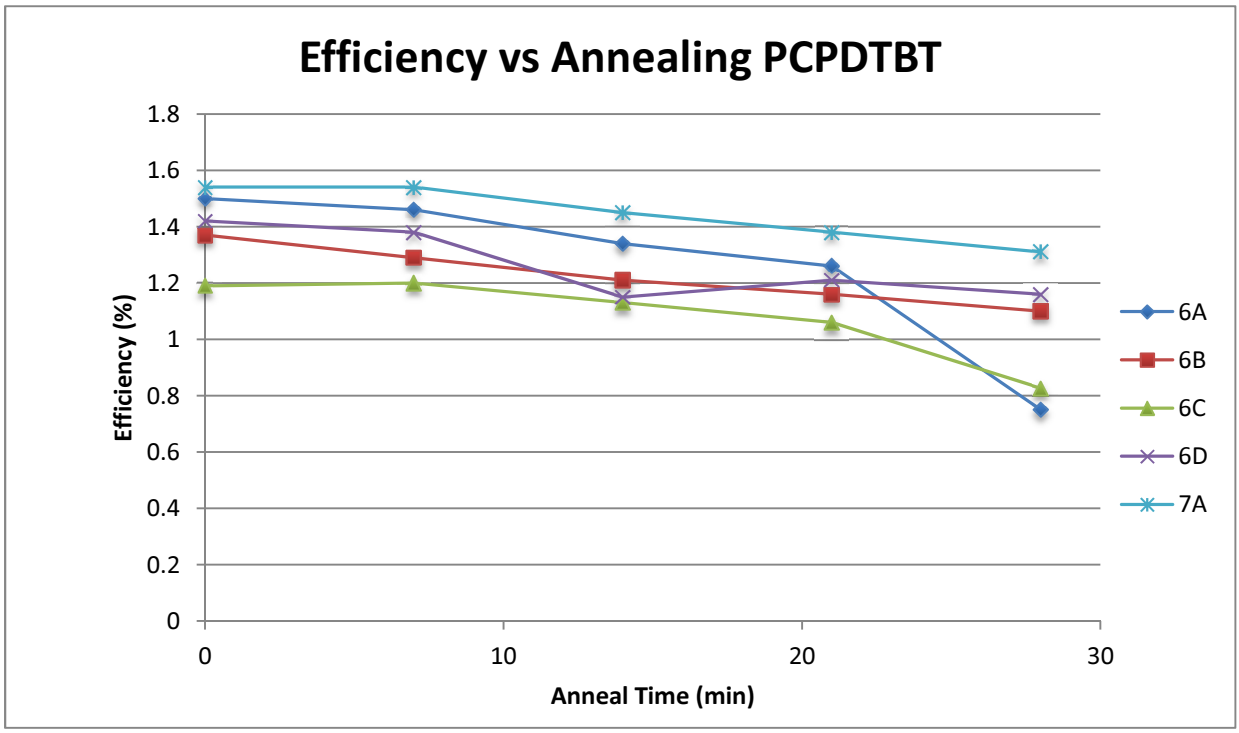

Figure 3b - Efficiency testing for PCPDTBT devices at 140 °C for 7 minute intervals. Devices all seem to drop from annealing, these results were not reproducible in the second PCPDTBT run but this may have been caused from an overly dissolved polymer layer or the higher temperature anneal.

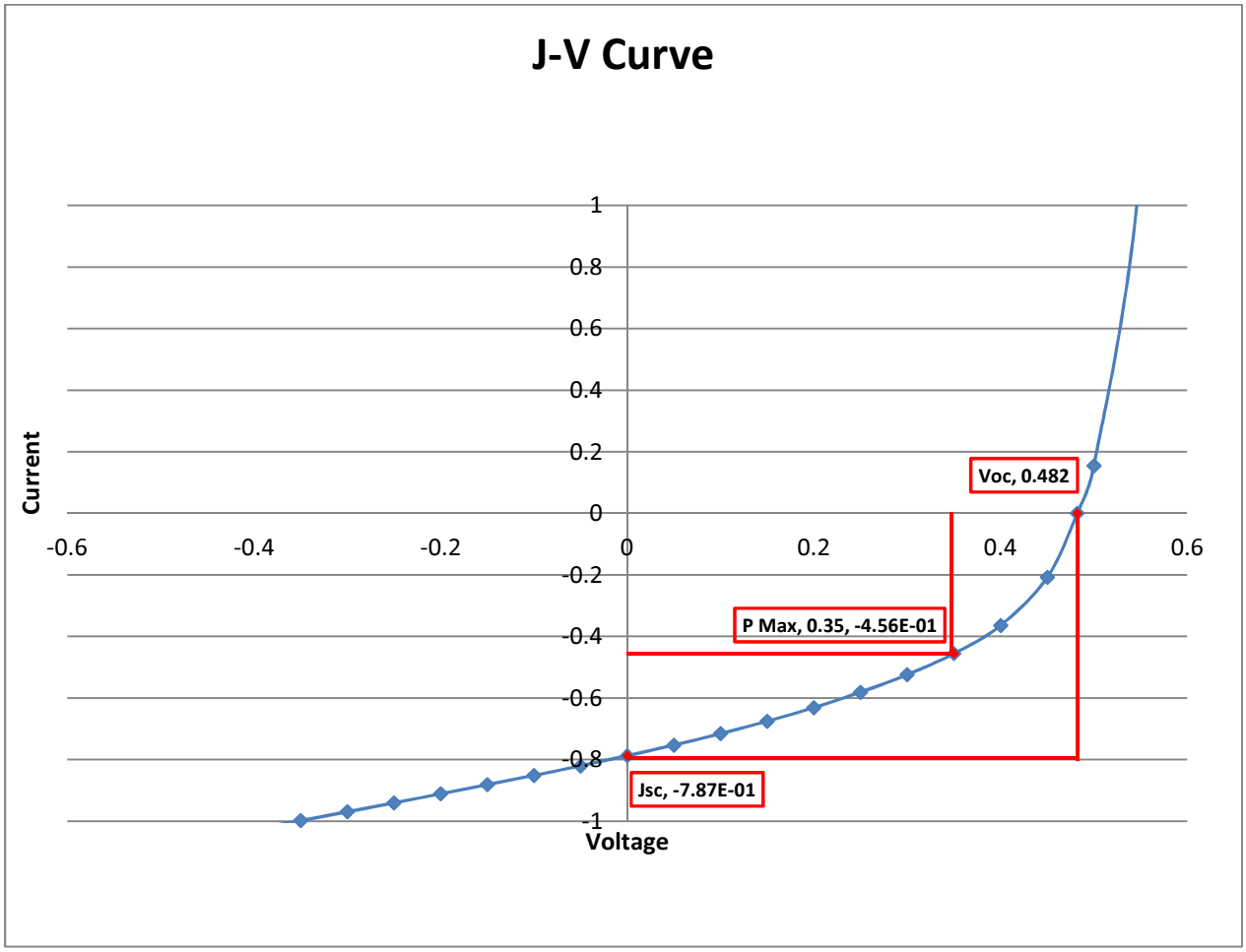

Figure 4 - J-V curve of a PCPDTBT device. The plot is scaled down to better represent the intersection of both axes. From a J-V curve we can calculate Jsc, Voc, Efficiency, and Fill Factor, see example calculations below:

$$Efficiency_{light} = \frac{Electrical\ Power_{max}}{Light\ Power_{input}} = \frac{0.35\ \text{V} * 0.456\ \frac{\text{A}}{\text{m}^2}}{18\ \frac{\text{w}}{\text{m}^2}} * 100\% = 0.886\%$$

$$Fill\ Factor = \frac{Power_{max}}{Jsc * Voc} = \frac{0.35\ \text{V} * 0.456\ \frac{\text{A}}{\text{m}^2}}{7.87 * 10^{-1}\ \frac{\text{A}}{\text{m}^2} * 0.482\ \text{V}} * 100\% = 42\%.$$

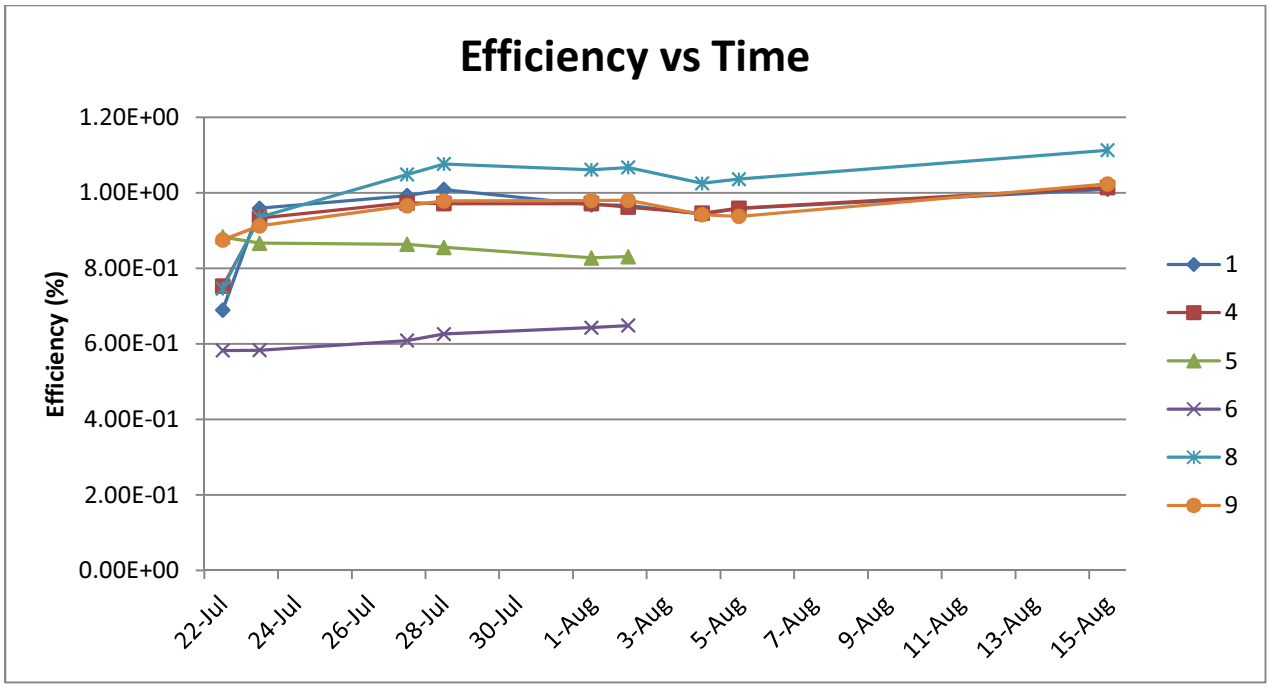

Figure 5a – Shows the efficiency of PCPDTBT and P3HT:PCPDTBT devices from the second run through time. Devices 5 and 6 were removed from the graph early because they were annealed. The rest of the devices can be found in Table 6.

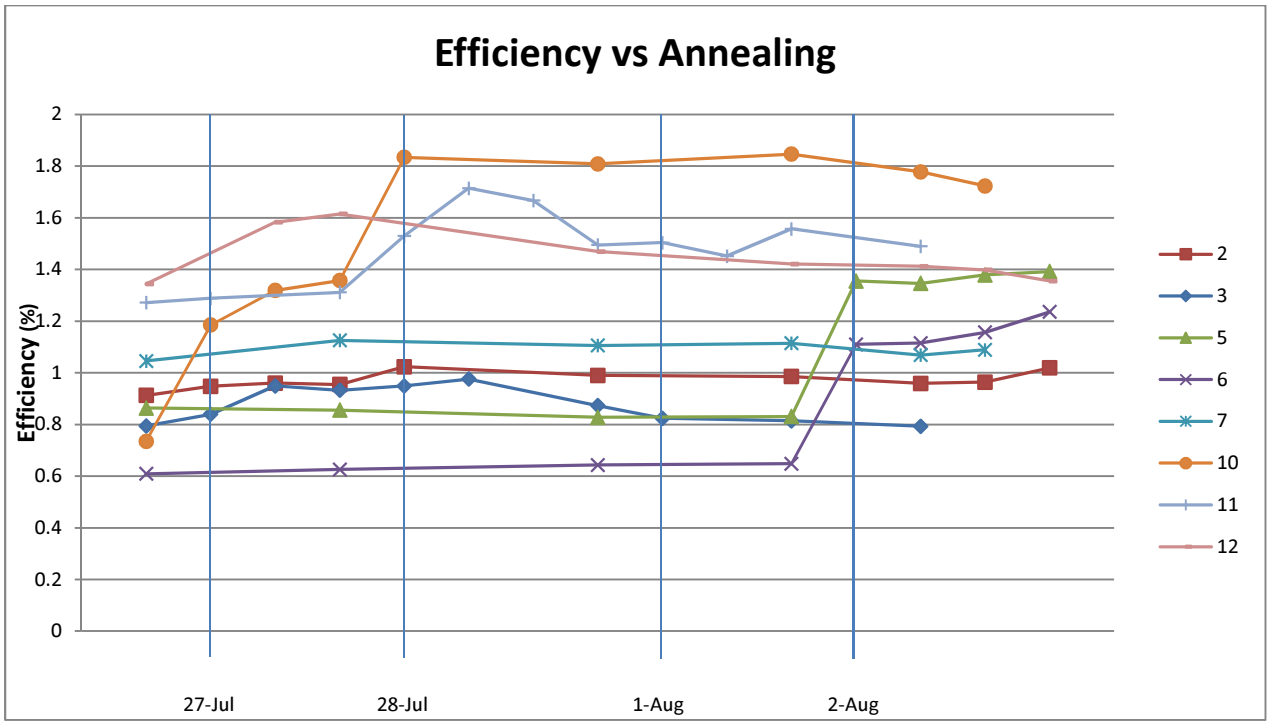

Figure 5 – Represents the effect of annealing on PCPDTBT and P3HT:PCPDTBT devices. The lines on certain dates represent the first anneal of the day while the markers represent the tests for a specific device. Some markers represent pre-anneal tests. Devices 5 and 6 were annealed last in accordance with Table 6 and showed significant improvement.

	Device	Spin Speed		Thermal Annealing	Date							
		2K	4K	No Pre-Cathode Anneal	27-Jul		28-Jul			1-Aug		2-Aug
					1st	2nd	1st	2nd	3rd	1st	2nd	
PCPDTBT	1	X										
	2	X			80	80	105					
	3	X			80	105	105	105		130		
	4	X										
PCPDTBT:P3HT	5	X										105 (25 min)
	6	X										130 (25 min)
PCPDTBT	7		X	X	80							
	8		X									
	9		X									
PCPDTBT:P3HT	10		X	X	80	80	105					
	11		X		80		105	105	105	105	130	
	12		X			105						

Table 6 - The different annealing and spin speed specifications for the second device run. All devices were annealed for 10 minutes except for the anneal of 5 and 6 on the 2nd of August as noted in the table.

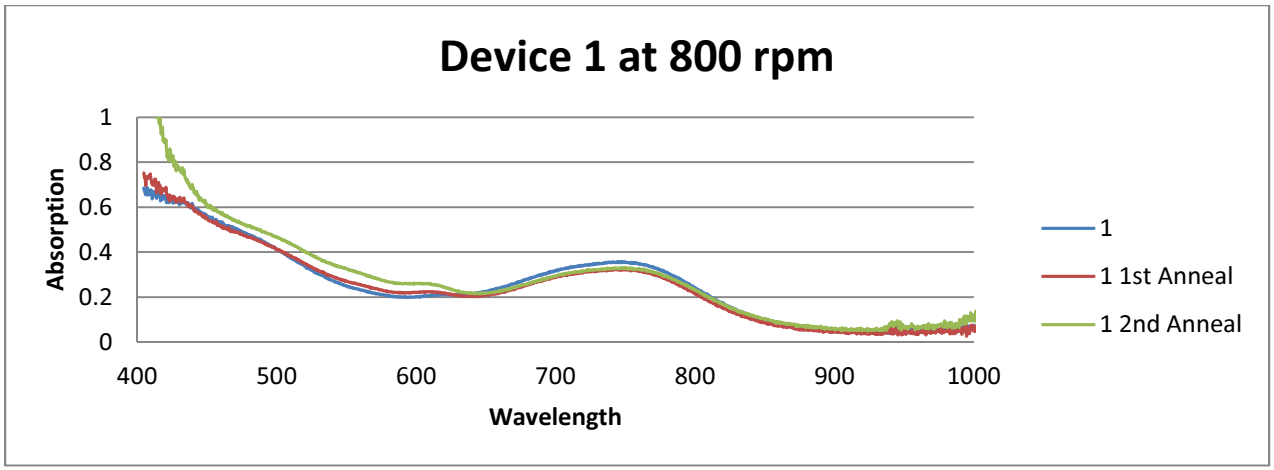

Figure 7a

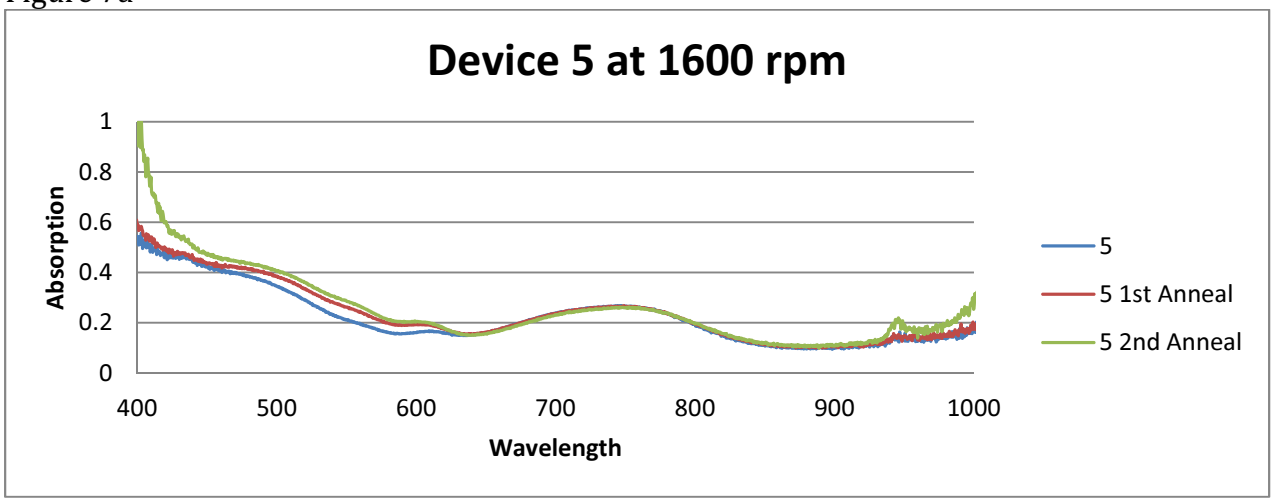

Figure 7b

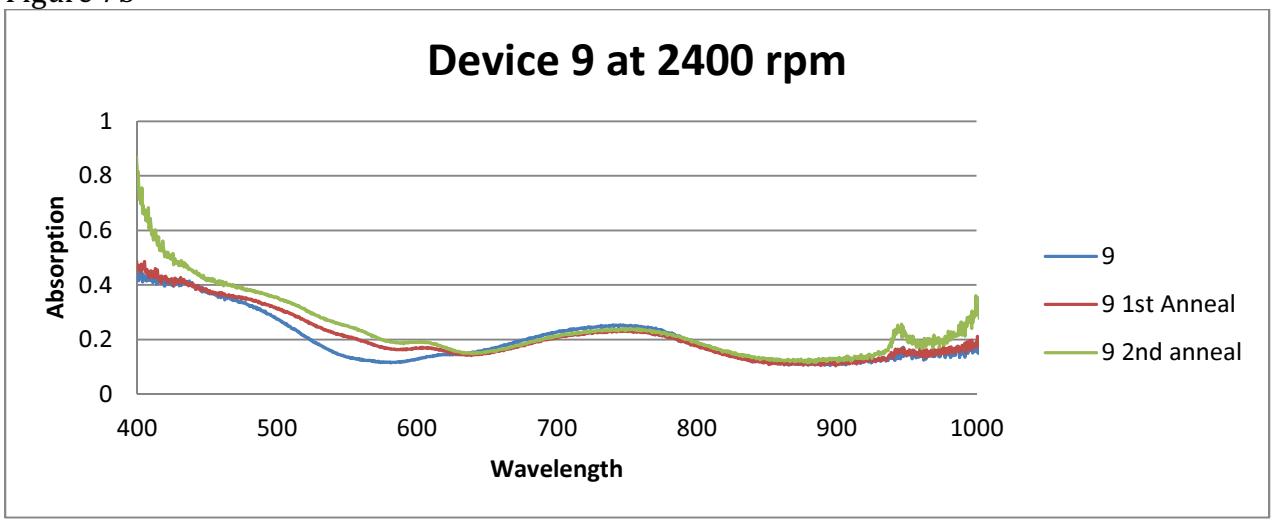

Figure 7c

Figure 7a-c – P3HT:PCPDTBT devices spun at various speeds (the slower the speed the thicker the layer and thus the higher the absorption). It is apparent that with annealing the absorption between 500 and 600 nm increases dramatically as the P3HT crystallizes and is thus able to capture more incoming light.

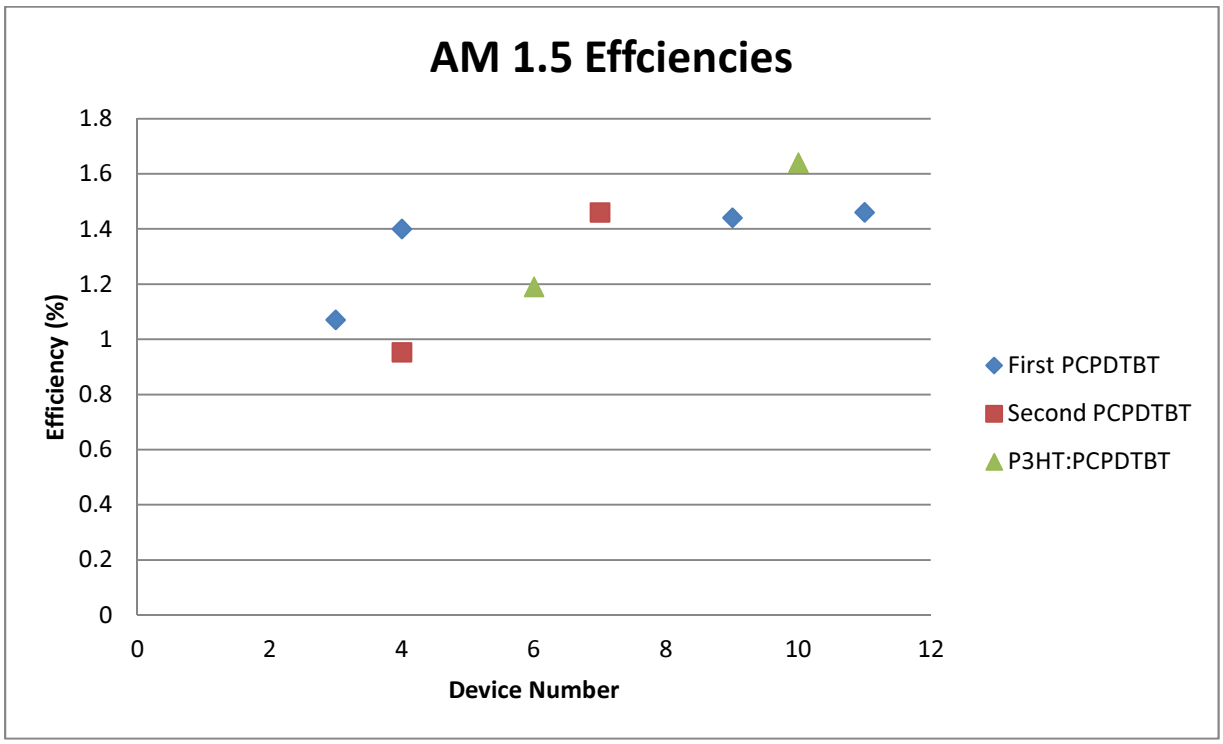

Figure 8 – Different devices from the first and second runs. Devices efficiencies were averaged over device pixels for this graph. Overall the first PCPDTBT run had higher efficiencies in AM 1.5 than the second PCPDTBT devices. The P3HT:PCPDTBT blend is on par if not better than the pure PCPDTBT devices. Furthermore the thinner devices performed better as charge extracting pathways need to span less distance to reach the device electrodes.